

1 Targeted mutagenesis using CRISPR-Cas9 in the chelicerate
2 herbivore *Tetranychus urticae*

3
4 Wannes Dermauw^a, Wim Jonckheere^a, Maria Riga^b, Ioannis Livadaras^b, John Vontas^{b,c}, Thomas
5 Van Leeuwen^a

6
7 ^aLaboratory of Agrozoology, Department of Plants and Crops, Faculty of Bioscience
8 Engineering, Ghent University, Coupure links 653, 9000, Ghent, Belgium

9
10 ^bMolecular Entomology Lab, Institute of Molecular Biology and Biotechnology (IMBB),
11 Foundation for Research and Technology (FORTH), Nikolaou Plastira Street 100, 70013,
12 Heraklion, Crete, Greece

13 ^cPesticide Science Laboratory, Department of Crop Science, Agricultural University of Athens,
14 Iera Odos 75, 11855, Athens, Greece

15
16
17
18

19 corresponding authors:

20 Wannes Dermauw (wannes.dermauw@ugent.be) and Thomas Van Leeuwen
21 (thomas.vanleeuwen@ugent.be)

22
23
24
25
26
27
28
29
30
31
32
33
34
35
36
37
38
39
40
41
42
43
44

45 **Abstract**

46

47 The use of CRISPR-Cas9 has revolutionized functional genetic work in many organisms,
48 including more and more insect species. However, successful gene editing or genetic
49 transformation has not yet been reported for chelicerates, the second largest group of
50 terrestrial animals. Within this group, some mite and tick species are economically very
51 important for agriculture and human health, and the availability of a gene-editing tool would
52 be a significant advancement for the field. Here, we report on the use of CRISPR-Cas9 to create
53 gene knock-outs in the spider mite *Tetranychus urticae*. The ovary of virgin adult females was
54 injected with a mix of Cas9 and sgRNAs targeting the phytoene desaturase gene. Natural
55 mutants of this gene have previously shown an easy-to-score albino phenotype. Albino sons
56 of injected virgin females were mated with wild-type females, and two independent
57 transformed lines were created and further characterized. Albinism inherited as a recessive
58 monogenic trait. Sequencing of the complete target-gene of both lines revealed two different
59 lesions at expected locations near the PAM site in the target-gene. Both lines did not
60 genetically complement each other in dedicated crosses, nor when crossed to a reference
61 albino line with a known genetic defect in the same gene. In conclusion, two independent
62 mutagenesis events were induced in the spider mite *T. urticae* using CRISPR-Cas9, providing
63 an impetus for genetic transformation in chelicerates and paving the way for functional
64 studies using CRISPR-Cas9 in *T. urticae*.

65

66 **Keywords:** Chelicerata, genome editing, CRISPR, Cas9 ribonucleoprotein (RNP), Acari

67

68

69

70

71

72

73

74

75

76

77

78

79

80

81

82

83

84

85

86

87

88

89 1 Introduction

90

91 Mites and ticks are members of the chelicerates, the largest group of terrestrial animals after
92 insects. *T. urticae* and other spider mites are important crop pests worldwide. This herbivore
93 species is at the extreme end of the generalist-to-specialist spectrum and can feed on a
94 staggering 1,100 plant species. Not surprisingly, it is currently reported as the ‘most resistant’
95 pest worldwide, as it developed resistance to more than 90 acaricides (Mota-Sanchez and
96 Wise, 2019; Van Leeuwen and Dermauw, 2016; Van Leeuwen et al., 2015). In 2011, a 90 Mb
97 high-quality Sanger-sequenced genome became available for this species (Grbic et al., 2011).
98 This allowed to disentangle some of the molecular mechanisms underlying resistance,
99 whether to man-made pesticides or plant secondary compounds. The extreme adaptation
100 potential of *T. urticae* was associated with specific gene expansions in known detoxification
101 enzyme families, such as cytochrome P450 monooxygenases, glutathione-S-transferases,
102 carboxyl-choline esterases, an unexpected repertoire of ABC and MFS transporters, and a
103 proliferation of cysteine peptidases (Dermauw et al., 2013a; Dermauw et al., 2013b; Grbic et
104 al., 2011; Santamaría et al., 2012). In addition, several genes acquired via horizontal gene
105 transfer were uncovered and characterized, such as intradiol-ring cleaving dioxygenases
106 (Schlachter et al., 2019; Wybouw et al., 2012; Wybouw et al., 2014; Wybouw et al., 2018).
107 Gene-expression studies have revealed large transcriptional differences between susceptible
108 and resistant *T. urticae* strains, as well as after short-term transfer or adaptation to new hosts
109 (Dermauw et al., 2013b; Grbic et al., 2011; Snoeck et al., 2018; Wybouw et al., 2014; Wybouw
110 et al., 2015; Zhurov et al., 2014). Furthermore, mite-plant interactions have been thoroughly
111 examined (Alba et al., 2015; Blaazer et al., 2018; Bui et al., 2018; Jonckheere et al., 2016;
112 Martel et al., 2015; Santamaría et al., 2019; Wybouw et al., 2015; Zhurov et al., 2014). For
113 instance, some salivary proteins were shown to modulate plant defenses (Iida et al., 2019;
114 Villarroel et al., 2016). The availability of a high-quality genome and new technical advances
115 in high-throughput sequencing has also led to the development of a genetic mapping tool,
116 bulked-segregant analysis, which allowed to map quantitative trait loci at high resolution
117 (Bryon et al., 2017; Kurlovs et al., 2019; Van Leeuwen et al., 2012; Wybouw et al., 2019a). To
118 conclude, the spider mite has been an exceptional good model to study adaptation, owing to
119 clear advantages in experimental manipulation, a small high-quality genome and the
120 development of advanced genomic mapping tools.

121

122 However, the lack of tools for reverse genetics that can directly validate the involvement
123 of genes and mutations in phenotypes of interest (and validate most of the work outlined
124 above) has impeded critical advances in *T. urticae* molecular biology. RNA interference (RNAi)
125 has dramatically accelerated scientific progress in different groups of insects (Scott et al.,
126 2013), linking genes with phenotypes, but this technique is currently not always
127 straightforward in mites (Kwon et al., 2016; Suzuki et al., 2017). Even more so, a recent
128 technique, named clustered regularly interspaced short palindromic repeats (CRISPR) -
129 CRISPR-associated protein 9 (Cas9), has revolutionized functional genetic work in many

130 organisms (Zhang and Reed, 2017). Successful CRISPR-Cas9-mediated gene manipulation has
131 been reported for a steadily increasing number of organisms in the arthropod subphyla
132 Crustaceae (Gui et al., 2016; Martin et al., 2016; Nakanishi et al., 2014) and Hexapoda,
133 including Diptera, Hymenoptera, Hemiptera, Coleoptera, Orthoptera and diverse Lepidoptera
134 (see Sun et al. (2017) for a review, Kotwica-Rolinska et al. (2019); Xue et al. (2018)), but not in
135 the wide group of chelicerates. It is clear that the development of such method for directed,
136 heritable gene editing is also crucial for the study of *T. urticae* and other mite and tick species.
137

138 The CRISPR-Cas9 technique currently usually consists of a two-component system with a
139 small, easy to synthesize single guide RNA (sgRNA) and a bacterial nuclease (Cas9). It
140 introduces double-stranded breaks in eukaryotic genomes, where the breaks can be repaired
141 randomly (non-homologous end-joining, NHEJ) or based on a template (homology-directed
142 repair) (Scott et al., 2018). In order to obtain efficient genomic DNA cleavage, Cas9 and sgRNA
143 should be introduced into the oocytes (Rungger et al., 2017). In *Drosophila*, this is currently
144 most easily accomplished by injecting sgRNAs in transgenic embryos expressing Cas9 under a
145 germline-specific promotor (see for example Bajda et al. (2017) and Douris et al. (2016), and
146 references in Korona et al. (2017)). Most current approaches with non-model organisms rely
147 upon delivering the Cas9 ribonucleoprotein (RNP) complex (Cas9 protein + sgRNA) by
148 embryonic microinjection (Chaverra-Rodriguez et al., 2018). However, within the chelicerates,
149 embryo injection has not been accomplished yet, as injected embryos die (Garb et al., 2018;
150 Sharma, 2017). This is probably the main reason why transgenic mites and ticks have not yet
151 been reported (with the exception of one older study that was never replicated (Presnail and
152 Hoy, 1992)). An alternative method, avoiding the injection of eggs or embryos, is delivery of
153 the RNP complex to the germline by injecting the mother animals. Such approaches already
154 proved to be successful for organisms such as nematodes (Witte et al., 2015) and insects
155 (Chaverra-Rodriguez et al., 2018; Hunter et al., 2018; Macias et al., 2019). In this study, we
156 used a similar approach, and injected virgin *T. urticae* females with a Cas9-sgRNA complex
157 targeting the *T. urticae* phytoene desaturase gene, a gene essential for red pigmentation
158 (Bryon et al., 2017; Bryon et al., 2013). Among the progeny, we identified albino males and
159 show that their albino phenotype was the result of Cas9-induced mutations in the phytoene
160 desaturase gene, hereby providing proof of principle of the feasibility of genetic modification
161 of mites and other chelicerates.

162 2 Material and Methods

163 2.1 *T. urticae* strain

164 The London strain (wild type, WT) of *T. urticae* is an outbred reference laboratory strain (Van
165 Leeuwen et al., 2012) and was used for sequencing of the complete *T. urticae* genome (Grbic
166 et al., 2011). All injection experiments were performed with mites from this strain. The Alb-
167 NL strain used in complementation tests was previously described (Bryon et al., 2017). All
168 strains were maintained as previously described (Riga et al., 2017) on *Phaseolus vulgaris* cv.
169 "Prelude" at 26±1°C, 60% RH and 16:8 (light:dark) photoperiod.

170 2.2 Recombinant Cas9 ribonucleoproteins and sgRNAs

171 Recombinant *Streptococcus pyogenes* Cas9 protein with an N-terminal nuclear localization
172 signal (NLS) (Alt-R® S.p. Cas9 Nuclease V3, catalog # 1081058) was purchased from Integrated
173 DNA Technologies (Leuven, Belgium). Two guide sequences were designed using the CRISPOR
174 website ((2018), accessed in December 2018), with the following settings: *T. urticae* phytoene
175 desaturase sequence (*tetur01g11270*,
176 <https://bioinformatics.psb.ugent.be/orcae/overview/Tetur>) as target (“Step 1”), *T. urticae*
177 London genome (GCA_000239435.1) as genome (“Step 2”) and “20 bp NGG – Sp Cas9” as
178 Protospacer Adjacent Motif (“Step 3”). Based on the guide DNA sequences, 3 nmol of single
179 guide RNAs (sgRNA) was ordered. The ordered sgRNAs were synthetic sgRNAs (sgRNA1 and
180 sgRNA2) from Synthego (Synthego Corporation, Menlo Park, California, USA), consisting of a
181 20 nt guide sequence (g1 or g2) + 80-mer “Synthego scaffold”

182 2.3 *In vitro* Cas9-sgRNA cleavage experiment

183 Before performing *in vivo* CRISPR-Cas9 experiments with *T. urticae*, we tested whether the
184 Cas9-sgRNA complex could cleave PCR products of *tetur01g11270* *in vitro*. Primer3 (Rozen and
185 Skaletsky, 2000) was used to design primers that amplify the *tetur01g11270* regions that are
186 targeted by the two sgRNAs (see above). An 895 bp region is amplified by the
187 “*tetur01g11270_DNA_1*” primers (amplicon 1, containing the sgRNA1 cutting site), while
188 “*tetur01g11270_DNA_2*” primers amplify a 699 bp region (amplicon 2, containing the sgRNA2
189 cutting site). *T. urticae* DNA was extracted from the WT strain using the Gentra Puregene
190 Tissue Kit (QIAGEN), according to the manufacturer’s instructions and using 100 adult females
191 as starting material. The PCR of *tetur01g11270* fragments (amplicon 1 and 2) was conducted
192 using the Expand™ Long Range dNTPack (Sigma-Aldrich). PCR reaction mixtures were
193 prepared according to the manufacturer’s instructions and using the following temperature
194 profile: denaturation for 2 min at 92°C, followed by five touch-down cycles of denaturation at
195 92°C for 10 s, annealing at 60°C -1°C/cycle for 15 s and elongation at 68°C for 1 min. Next, 37
196 cycles of 92°C for 10 s, 55°C for 15 s and 68°C for 1 min. After a final elongation of 68°C for 5
197 min, PCR products were checked by agarose gel electrophoresis, and purified using the EZNA®
198 Cycle Pure Kit (Omega Bio-Tek). The *in vitro* digestion protocol was performed as described by
199 the IDT Alt-R CRISPR-Cas9 System Protocol (version September 2019, available at
200 <https://eu.idtdna.com/pages/support/guides-and-protocols>, document ID# CRS-10096-PR
201 09/19), with some modifications. Briefly, the RNP complex was created by combining 2.5 µl
202 sgRNA (10 µM stock in TE buffer, pH 7.5), 0.4 µl Alt-R S.p. Cas9 enzyme (62 µM stock) and 22.1
203 µl Cas9 dilution buffer (30 mM HEPES, 150 mM KCl, pH 7.5). For negative controls, sgRNA was
204 replaced by TE. After incubation for 10 min at RT, the *in vitro* digestion reaction was assembled
205 at RT as follows: 2 µl 10x Cas9 Nuclease Reaction Buffer (200 mM HEPES, 1 M NaCl, 50 mM
206 MgCl₂, 1 mM EDTA, pH 6.5), 4 µl Cas9 RNP (from previous step), 10 µl DNA substrate (amplicon
207 1 or 2, 50 nM stock) and 4 µl of water. The reaction mixture was incubated for 90 min at 37°C,
208 after which 2 µl proteinase K (Sigma-Aldrich; 10 mg/ml) was added, and the DNA substrate
209 was released from the Cas9 endonuclease by incubating for 10 min at 56°C. Subsequently, the

210 digestion was analyzed using gel electrophoresis, in which 15 μ L reaction mixture was loaded
211 on gel.

212 2.4 *In vivo* Cas9-sgRNA cleavage experiment

213 2.4.1 Cas9-sgRNA injection mix

214 The Cas9-sgRNA injection mix was prepared as indicated in Table S1. The final concentration
215 of the Cas9 protein in the injection mix was 4.85 μ g/ μ L (29.61 μ M). Stock solution of each
216 sgRNA was prepared by dissolving 3 nmol of sgRNA into 30 μ L of RNase-free water. sgRNAs
217 were added to the injection mix in a 1:3 Cas9:sgRNA molar ratio and 0.5 mM of chloroquine
218 was also included in the injection mix. The Cas9-sgRNA injection mix was incubated at 37°C
219 for 10 min, and finally, the injection mix was centrifuged at 4°C for 10 min at 10,000 g and
220 kept on ice until injection.

221 2.4.2 Injection of *T. urticae* female mites

222 Female mites of the WT strain were allowed to lay eggs on the upper part of bean leaves on
223 wet cotton in a Petri dish. After eight days, teliochrysalis females were transferred to another
224 leaf disk and allowed to molt. After another one to four days, these unfertilized females were
225 used for injections. Agar plates were made by dissolving 15 g of agar into 500 mL of cherry
226 juice (for color contrast, brand “Eviva”) and subsequently heated until boiling. An agar
227 “platform” was made by adding two glass microscope slides (26 x 76 mm, 1.1 mm thick;
228 APTACA, Canelli, Italy), attached to each other by double-sided tape, into a Petri dish
229 immediately after pouring the agar plates. After solidification of the agar, the microscope
230 slides were removed, and the agar plate was cut in two along the length of the microscope
231 slide (Figure S1). Unfertilized females were aligned on the agar platform, with their dorsal and
232 right lateral side in contact with the agar (Figure 1). Injection needles were pulled from Clark
233 capillary glass (borosilicate with filament: 1.0 mm (outside diameter, OD) x 0.58 (inner
234 diameter, ID) x 100 mm (length); catalog # W3 30-0019/GC100F-10 (Harvard Apparatus Ltd,
235 Holliston, Massachusetts, USA)) using a P97-micropipette needle puller (Sutter Instruments,
236 Novato, California, USA), with the following settings “Heat: 510, Pull: 20, Velocity: 90, Time:
237 250” (Figure S2). Mites were injected under a Leitz BIOMED Microscope (Wild Leitz/Leica,
238 Wetzlar, Germany) and with a mechanical micromanipulator (Leitz/Leica, Wetzlar, Germany)
239 that holds the injection needle (Figure 1). Approximately 6 nl of Cas9-sgRNA injection mix was
240 injected in the ovary, near the third pair of legs, using a IM 300 Microinjector (Narishige,
241 London, UK). Two batches (A and B) of mites were injected. Each batch of injected mites was
242 transferred to a separate leaf disk and allowed to lay eggs. After 24 hours, the injected females
243 were transferred to a new leaf disk and allowed to lay eggs again. The male haploid progeny
244 of injected females (on six leaf disks in total (2 batches: A and B, 2 time-points: 0-24h and 24-
245 48h)) was visually screened for the albino phenotype beginning 3 days after egg deposition.

246 2.5 Mode of inheritance of albino phenotype and generation of homozygous albino CRISPR
247 lines A and B.

248 Albino sons from RNP-injected females from the A and B batch were isolated on bean leaf
249 disks (one male per leaf disk) and allowed to mate with three to five virgin females of the
250 parental strain (London, WT). Mated females were allowed to lay eggs for six days on the leaf
251 disk (disk 1) and were discarded afterwards. Next, three F₁ teliochrysalis females that
252 developed from eggs on disk 1, were transferred to a separate leaf disk, allowed to hatch, and
253 to lay eggs for four days (disk 2). These virgin F₁ females (from disk 2) were then transferred
254 to another leaf disk and kept at 10°C to increase their life span (disk 3). Subsequently, the
255 number of albino and WT males was counted on disk 2 and an albino male from disk 2 was
256 mated with its virgin mother (on disk 3) to generate a homozygous albino line (CRISPR lines A
257 and B). For these two lines, we also performed a complementation test on detached bean
258 leaves. Briefly, 15 virgin (teliochrysalis) females from CRISPR line A or B were crossed with 30
259 males from the Alb-NL strain (Bryon et al., 2017). At least 100 resulting F₁ females were
260 assessed for albinism. Last, we also performed a complementation test between 15
261 teliochrysalis females of CRISPR line A and 30 males of CRISPR line B, and scored albinism for
262 at least 100 F₁ females.

263 2.6 DNA and RNA extraction from *T. urticae* CRISPR lines A and B and PCR amplification of
264 *tetur01g11270*

265 DNA was collected from five pooled females from lines A and B using the CTAB method
266 previously described by Navajas et al. (1998). PCR of *tetur01g11270* fragments was performed
267 using the primers of the *in vitro* Cas9-sgRNA cleavage experiment (Table S1) and extracted
268 DNA from lines A and B was used as template. The reactions consisted of 3 µl 10x Buffer, 0.2
269 mM of each dNTP, 0.33 µM of each primer, 2 µl template, 1U Kapa Taq DNA Polymerase (Kapa
270 Biosystems) in a final volume of 30 µl and with cycling conditions as follows: 5 min at 95°C
271 followed by 40 cycles of 30 s at 95°C, 40 s at 53°C, 1 min at 72°C and a final extension of 2 min
272 at 72°C. PCR amplicons were verified on a 1.5% agarose gel, purified using the NucleoSpin®
273 Gel and PCR Clean-Up kit (Macherey-Nagel) according to the manufacturers' instructions.
274 Nucleotide sequences were determined in both strands of purified PCR products at the CeMIA
275 sequencing facility (CEMIA, SA., Greece). Finally, RNA was extracted from mites of the A and
276 B line. About 100 females were collected and RNA was extracted using the Qiagen RNeasy
277 PLUS Kit (Qiagen Benelux, Venlo, Nederland). One µg of total RNA was used as template for
278 synthesizing cDNA with the Maxima First Strand cDNA synthesis Kit for RT-qPCR (Fermentas
279 Life Sciences, Aalst, Belgium). Primer3 (Rozen and Skaletsky, 2000) was used to design primers
280 (*tetur01g11270_cDNA* primers) that amplify the coding sequence of the phytoene desaturase
281 gene (*tetur01g11270*) (Table S1. PCRs were performed using the Expand Long Range dNTP
282 Pack (Roche/Sigma-Aldrich, Belgium). Reaction mixtures were prepared according to the
283 manufacturer's instructions. The thermal profile consisted of denaturation for 2 min at 92°C,
284 followed by 4 touch-down cycles of denaturation at 92°C for 10 s, annealing at 57°C -1°C/cycle
285 for 15 s and elongation at 68°C for 2.5 min. Next, 40 cycles of 92°C for 10 s, 53°C for 15 s and

286 68°C for 2.5 min. After a final elongation of 68°C for 7 min, PCR products were purified using
287 the E.Z.N.A. Cycle Pure kit (Omega Biotek) and Sanger sequenced by LGC genomics (Germany)
288 with forward and reverse primers and four internal primers (Table S1).

289 2.7 Imaging

290 Images of adult females and immature stages of *T. urticae* were taken with an Olympus OM-
291 D E-M1 mark II using a micro-objective on bellows (Nikon PB- 4). The following micro-
292 objectives were used: a Nikon M Plan 10x 160/0.25 (for females and larvae of WT strain and
293 CRISPR line A), Nikon achromatic 10x 160/0.25 (for females of CRISPR line B) and a Nikon BD
294 Plan ELWD 20x 210/0.4 (for larvae of CRISPR line B). Between 50-150 pictures were used for a
295 focus stack. The open-source software `align_image_stack`
296 (https://www.systutorials.com/docs/linux/man/1-align_image_stack/) and `Enfuse`
297 (<http://software.bergmark.com/enfuseGUI/Main.html>) were used to generate the focus
298 stack, while `Darktable` (<https://www.darktable.org/>) was used for pre-and posttreatment of
299 images. Images of adult males were taken using a stereomicroscope (Leica S8 Apo, Witzlar
300 Germany) and a Leica DFC295 camera.
301

302 3 Results

303 3.1 sgRNA guide sequence design and *in vitro* Cas9-sgRNA cleavage

304 Guide sequences were designed using the CRISPOR website as described above. The first guide
305 sequence (g1, 5'-GGTGGCAAGAGCACGAGCAC-3') was selected because it had the highest
306 "out-of-frame" score (the higher this score, the more deletions have a length that is not a
307 multiple of three (Bae et al., 2014)) while the other guide sequence (g2, 5'-
308 ACAATGGGTACTCCAGTACC-3') was selected because it was located in a region postulated to
309 encode the carotenoid binding domain of the phytoene desaturase (Armstrong et al., 1989;
310 Sanz et al., 2002). Finally, both guide sequences had a predicted off-target count of zero. *In*
311 *vitro* Cas9-sgRNA cleavage of PCR amplicons of *tetur01g11270* resulted in the correct *in silico*-
312 predicted digestion pattern: amplicon 1 (895 bp) was cleaved into a 537 and 398 bp fragment,
313 while amplicon 2 (699bp) was cleaved into a 197 bp and 502 bp fragment (Figure S3).

314 3.2 *In vivo* Cas9-sgRNA experiment

315 3.2.1 Screening of albino male progeny and generation of CRISPR lines A and B

316 Two batches of virgin females were injected in the ovary: 245 mites in batch "A" and 177 mites
317 in batch "B". Twenty-four hours after injection, the percentage of alive females was recorded
318 as 78.4% and 71.8%, respectively. Injected females were allowed to lay eggs for 24h, were
319 placed on new arenas, and allowed to lay eggs for another 24 hours. The number of eggs on
320 each arena was, approximately, 650 and 900 for batch A and 260 and 650 for batch B after 24
321 h and 24-48 h, respectively. After hatching, we screened for male larvae lacking pigment. In
322 the arenas with eggs deposited within 24 hours after injection, we found one alive albino male

323 in both batch A and B (Table 1), while in batch A thirteen specimens with albino phenotype
324 were detected in larvae/protochrysalises resulting from eggs deposited between 24 and 48
325 hours after injection. However, none of these larvae/protochrysalises developed into adults.
326 From both batches, the alive albino male was isolated, allowed to develop to the adult stage
327 and crossed to obtain homozygous stable lines named CRISPR line A and B, respectively, which
328 were characterized further. All life stages of CRISPR line A lacked red pigments (Figure 3, Figure
329 S4). In contrast, only immature stages lacked red pigmentation in CRISPR line B, while adult
330 stages do show traces of red pigmentation in the eyes, especially visible in the males, but lack
331 red pigmentation in the forelegs (Figure 3, Figure S4, Figure S5).

332 3.2.2 Mode of inheritance and complementation test of albino phenotype in CRISPR lines A 333 and B

334 The genetic basis of the albino phenotype found in males of CRISPR lines A and B was
335 determined by crossing line A and B males with females of the original WT strain. In all cases,
336 F₁ females of the resulting cross had normal body and eye color (Table 2). Together with the
337 finding of an approximate 1:1 ratio of albino to WT phenotype in haploid F₂ sons produced by
338 virgin F₁ females, this strongly indicated that albinism was inherited as a monogenic recessive
339 trait. In a complementation test, females of CRISPR line A and males of CRISPR line B were
340 crossed, and the resulting F₁ females were all albinos indicating that the albino phenotype in
341 both lines is caused by a disruption in the same gene (Table 2). Finally, we also crossed females
342 of CRISPR lines A and B with males of strain Alb-NL, known to have an inactivating mutation
343 in the phytoene desaturase gene (*tetur01g11270*) (Bryon et al. 2017), and found that all
344 female F₁ progeny was albino. This failure to complement suggests that the albino phenotype
345 of CRISPR lines A and B results from a mutation or disruption in *tetur01g11270*, the gene
346 targeted by our Cas9-sgRNA experiment.

347 3.2.3 Sequence analysis of *tetur01g11270* in CRISPR lines A and B

348 DNA was extracted from CRISPR lines A and B and sequencing of PCR amplicons 1 and 2
349 revealed disruptions in the *tetur01g11270* gene in both lines. *Tetur01g11270* of CRISPR line B
350 harbored a 6 bp deletion (nt 1117-1122 in WT reference sequence of *tetur01g11270*) that was
351 located 6 bp upstream of the sgRNA1 PAM site, causing a loss of two amino acids (Arg406 and
352 Ala407).

353 Based on an alignment of phytoene desaturases of insects, fungi and bacteria (Figure 3d)
354 Arg406 is highly conserved. CRISPR line A harbored a 7 bp deletion (nt 1444-1450 in
355 *tetur01g11270* in WT reference sequence of *tetur01g11270*) that was located 4 bp upstream
356 of the sgRNA2 PAM site, resulting in the loss of two amino acids and a frame shift, changing
357 translation (Figure 3b) in the region of the carotenoid binding domain (Armstrong et al., 1989).
358 To assure that the detected deletions were the only disruptions in the coding sequence of
359 *tetur01g11270* of CRISPR lines A and B, we sequenced the complete cDNA sequence of
360 *tetur01g11270* of both CRISPR lines and the WT strain. The cDNA sequence of CRISPR line B
361 was, except for the 6 bp deletion, 100% identical to that of the WT strain, while in the cDNA
362 sequence of CRISPR line A, we found, next to the 7 bp deletion, three non-synonymous single

363 nucleotide polymorphisms (SNPs) (Figure S6). All three non-synonymous SNPs resulted in
364 favored substitutions according to Russel et al. (2003). The amino acid changes “K->Q” and “I-
365 >V” (Figure S6), caused by two non-synonymous SNPs, occur at a non-conserved amino acid
366 position in the phytoene desaturase protein (Figure S6 and Supplemental Figure S5 in Bryon
367 et al. Bryon et al. (2017)) and were also present in the WT strain at low frequency (data not
368 shown). Last, the remaining non-synonymous SNP (resulting in an amino acid change “V->I”)
369 was located downstream of the 7 bp deletion.

370 4 Discussion

371
372 CRISPR-Cas9 has revolutionized genome editing in metazoan species, including more and
373 more arthropods (Kotwica-Rolinska et al., 2019; Reardon, 2019; Sun et al., 2017). For many
374 arthropods, the ortholog of the *Drosophila white* gene, an ABC-transporter essential for eye
375 pigmentation, has been used as a CRISPR-Cas9 target for establishing proof of principle of this
376 technology (Bai et al., 2019; Ismail et al., 2018; Khan et al., 2017; Xue et al., 2018). For
377 chelicerates, such as mites and ticks, however, the CRISPR-Cas9 technology has not yet been
378 validated. The main reason is probably because the injection of mite and tick embryos is
379 currently not feasible (Khila and Grbić, 2007; Sharma, 2017) and because non-lethal
380 convenient genetic markers with a clearly visible phenotype are not yet available. In the two-
381 spotted spider mite *T. urticae*, for example, a clear ortholog of the *white* gene could not be
382 identified (Dermauw et al. 2013). However, recent studies have uncovered several mutations
383 that result in pigmentation defects in a number of spider mite populations and species (Bryon
384 et al., 2017; Wybouw et al., 2019b). For example, in *T. urticae*, it was shown that several
385 mutations in a gene encoding a phytoene desaturase (*tetur01g11270*) caused an albino
386 phenotype (lack of red pigment in frontal legs and eyes) (Bryon et al., 2017). Interestingly, like
387 in a few other arthropods (Zhao and Nabity, 2017), this gene was horizontally acquired from
388 fungi (Altincicek et al., 2012; Grbic et al., 2011) and encodes an enzyme that catalyzes the
389 formation of lycopene, from which β -carotene and other red pigments are derived (Maoka,
390 2019). The discovery of a *T. urticae* genetic marker with a clearly visible phenotype, scorable
391 in larvae and even embryos, significantly facilitates screening for potential genetic
392 transformants. We therefore took advantage of this discovery to design a CRISPR-Cas9
393 strategy with sgRNAs that target the phytoene desaturase of *T. urticae* (Figure 3). Next to the
394 availability of a genetic marker with a clearly visible phenotype, efficient CRISPR-Cas9 further
395 requires the delivery of the Cas9-sgRNA complex into the embryos in early development. As
396 successful injection of mite and tick embryos has currently not been achieved (see above), we
397 followed a strategy previously applied for nematodes, mosquitoes and psyllids (Chaverra-
398 Rodriguez et al., 2018; Cho et al., 2013; Hunter et al., 2018; Macias et al., 2019), and we
399 injected *T. urticae* females in the ovary, assuming that the Cas9-sgRNA complex would be
400 incorporated into the oocytes and developing embryos. In addition, the arrhenotokous
401 reproduction system allowed us to inject unfertilized females of which the progeny consists

402 of haploid males only. This allowed to immediately screen for an albino phenotype among the
403 male progeny of injected females.

404 In this study, two batches (A and B) of virgin *T. urticae* females were injected with Cas9-
405 sgRNA and in each batch one albino male was identified in the progeny developed from eggs
406 laid by females less than 24 hours after injection (Table 1). Subsequently, homozygous albino
407 lines (CRISPR line A and B) were generated from these males and both the mode of inheritance
408 and the complementation test revealed that disruptions in *tetur01g11270* caused the albino
409 phenotype (Table 2). The *T. urticae* genome harbors three copies of phytoene desaturase, and
410 although *tetur01g11270* is the only one with a clear role in pigment synthesis (Bryon et al.,
411 2013), one could question whether other *T. urticae* phytoene desaturase genes
412 (*tetur11g04820* and *tetur11g04810*, Grbić et al. (2011)) were also targeted. However,
413 complementation tests with a characterized albino line point to a single causal gene (Table 2).
414 In addition, no off-target effects were predicted for guide sequences of both sgRNAs, and
415 guide sequence regions differ significantly between *tetur01g11270* and the other two
416 phytoene desaturase genes (Figure S7). Further, to assess whether the *tetur01g11270*
417 disruptions were caused by typical CRISPR-Cas9 events, we sequenced *tetur01g11270* of
418 CRISPR lines A and B at the DNA and cDNA level. Typical CRISPR-Cas9 events (Jinek et al., 2012)
419 were identified in *tetur01g11270* of both lines, with deletions located four to six base pairs
420 upstream of the PAM site (Figure 3). Sequencing of the *tetur01g11270* full-length coding
421 sequence revealed that no other polymorphisms could be detected in CRISPR line B compared
422 to the WT strain, while the *tetur01g11270* coding sequence of CRISPR line A did contain three
423 favored non-synonymous mutations (Figure S6) of which two were also present in the WT
424 strain. Altogether, this leaves no doubt that the Cas9-induced deletions in *tetur01g11270* of
425 CRISPR lines A and B are the underlying genetic basis of the albino phenotype. Subtle
426 differences in the albino phenotype of each line could to some extent also be linked to the
427 type of the Cas9-sgRNA induced deletion. In CRISPR line A, the 7 bp deletion in *tetur01g11270*
428 causes a frameshift, thereby abolishing the carotenoid binding domain (Armstrong et al.,
429 1989), resulting in the lack of pigment in all stages. In CRISPR line B, the 6 bp deletion results
430 in the loss of two amino acids, including a highly conserved arginine, but does not change
431 translation (Figure 3d). While immature stages of CRISPR line B lack pigmentation, the eyes of
432 adult females and especially males of CRISPR line B, traces of red pigmentation could be
433 observed, suggesting the 6 bp deletion can be considered as a hypomorphic mutation, i.e.
434 causing only a partial loss of gene function (Muller, 1932).

435 Based on the total number of eggs that was laid by the injected females (1550 and 910
436 for batches A and B, respectively), the percentage of CRISPR-Cas9 transformed mite embryos
437 is low (Table 1). Especially when compared to the CRISPR-Cas9 efficiency in nematodes, where
438 a mutation frequency of up to 17% in the F₁ progeny can be obtained by injection of the Cas9-
439 sgRNA complex into the gonads (Cho et al., 2013). Furthermore, in contrast to the 24h egg
440 arenas of batch A and B, we could not obtain alive albino males from the 24-48h egg arena of
441 batch A, as all thirteen detected albino larvae/protochrysalises did not develop into
442 adulthood. Although genetic evidence was not gathered, we can assume that the observed

443 albino males with identical phenotype in interval 24-48h were caused by CRISPR-Cas9 events.
444 If this is the case, the decreased survival of the larvae/protochrysalises might have been the
445 result of multiple accompanying off-target CRISPR-Cas9 events at this time point after
446 injection. However, given that the CRISPOR software predicted that both sgRNAs have zero
447 off-target effects, this seems unlikely. If only the 24h time point is taken into consideration,
448 we obtained about one transformant per 200 injected females, a frequency that does allow
449 to screen for visible phenotypic traits immediately. Arrhenotokous reproduction allows to
450 immediately screen the males that can be directly used in dedicated crosses to fix the
451 mutation. Which time point after injection is the most likely to result in CRISPRed embryos
452 should be investigated and optimization of this timing could potentially increase screening
453 efficacy. Because of this straightforward phenotype screening and mutation fixation, a ‘CO-
454 CRISPR’ approach might be used to make this strategy also feasible for mutations without a
455 visible phenotype. In this approach, injection mixtures would contain sgRNA for both a marker
456 gene and additional target-gene. It was previously shown for nematodes that transformants
457 with the visible marker have a much higher frequency of mutations in the target-gene
458 (Dickinson and Goldstein, 2016; Farboud et al., 2019). This allows to preselect a number of
459 progeny for further screening.

460 Previously, Bryon et al. (2017) used a similar CRISPR-Cas9 approach in an attempt to
461 provide functional evidence of the role of mutations and deletions in *tetur01g11270* in
462 albinism. However, typical CRISPR-Cas9 events were not recorded. We hypothesized that this
463 was most likely due to insufficient RNP uptake by the oocytes. Here, we increased the Cas9
464 protein concentration more than 5-fold to 4.85 µg/µl. Furthermore, we also added
465 chloroquine, because it was recently shown that the addition of this compound improves
466 CRISPR-Cas9 efficiency in mosquitoes (Chaverra-Rodriguez et al. 2018). Recent studies also
467 hint toward other modifications that could improve CRISPR-Cas9 transformation efficiency,
468 such as the use of other adjuvants like lipofectamine or branched amphiphilic peptide
469 capsules (BAPC) (Adams et al., 2019; Hunter et al., 2018), or a shorter Cas protein (Rusk, 2019).
470 Last, in a recent breakthrough study it was shown how ReMOT (Receptor-Mediated Ovary
471 Transduction of Cargo) can be exploited to deliver Cas9 in oocytes after the injection of female
472 mosquitoes. In this system, a “guide peptide” (P2C) mediates the transduction of the Cas9
473 RNP complex from the female mosquito hemolymph to developing oocytes. Although the
474 principle of transformation should be transferable to other organisms, the peptide and
475 protein identified in Chaverra-Rodriguez et al. (2018) have no homologs outside dipterans
476 (flies and mosquitoes) and might not be readily transferable to mites and ticks.

477 In conclusion, two independent mutagenesis events were induced in the spider mite
478 *T. urticae* using CRISPR-Cas9, providing an impetus for genetic transformation in chelicerates
479 and paving the way for functional studies using CRISPR-Cas9 in *T. urticae*.

480

481 **Author contributions**

482 WD and TVL designed experiments; WD, WJ, MR and IL performed experiments. WD and TVL
483 wrote the manuscript, with input from JV, MR and WJ. All authors reviewed the manuscript.

484

485 **Acknowledgements**

486 We thank Merijn Kant (University of Amsterdam, The Netherlands) for providing the Alb-NL
487 strain, Gilles San Martin (Walloon Agricultural Research Centre CRA-W, Gembloux, Belgium)
488 for taking photographs (Figure 2, Figure S4) of the different spider mite lines, Astrid Bryon
489 (University of Wageningen, The Netherlands) for providing Figure 1a and René Feyereisen
490 (University of Copenhagen, Denmark/ University of Ghent, Belgium) for critical reading of the
491 manuscript. This work was supported by the European Union's Horizon 2020 research and
492 innovation program [grant 772026-POLYADAPT to TVL and 773902-SuperPests to TVL and JV].
493 During this study WD was a postdoctoral fellow of the Research Foundation Flanders (FWO).

494

495 **References**

496

497 Adams, S., Pathak, P., Shao, H., Lok, J.B., Pires-daSilva, A., 2019. Liposome-based transfection
498 enhances RNAi and CRISPR-mediated mutagenesis in non-model nematode systems. *Sci Rep*
499 *9*, 483.

500

501 Alba, J.M., Schimmel, B.C.J., Glas, J.J., Ataide, L.M.S., Pappas, M.L., Villarroel, C.A., Schuurink,
502 R.C., Sabelis, M.W., Kant, M.R., 2015. Spider mites suppress tomato defenses downstream of
503 jasmonate and salicylate independently of hormonal crosstalk. *New Phytol* *205*, 828-840.

504

505 Altincicek, B., Kovacs, J.L., Gerardo, N.M., 2012. Horizontally transferred fungal carotenoid
506 genes in the two-spotted spider mite *Tetranychus urticae*. *Biology Letters* *8*, 253-257.

507

508 Armstrong, G.A., Alberti, M., Leach, F., Hearst, J.E., 1989. Nucleotide sequence, organization,
509 and nature of the protein products of the carotenoid biosynthesis gene cluster of
510 *Rhodobacter capsulatus*. *Molecular and General Genetics MGG* *216*, 254-268.

511

512 Bae, S., Kweon, J., Kim, H.S., Kim, J.-S., 2014. Microhomology-based choice of Cas9 nuclease
513 target sites. *Nat Meth* *11*, 705-706.

514

515 Bai, X., Zeng, T., Ni, X.-Y., Su, H.-A., Huang, J., Ye, G.-Y., Lu, Y.-Y., Qi, Y.-X., 2019. CRISPR/Cas9-
516 mediated knockout of the eye pigmentation gene white leads to alterations in colour of
517 head spots in the oriental fruit fly, *Bactrocera dorsalis*. *Insect Mol Biol* *28*, 837-849.

518

519 Bajda, S., Dermauw, W., Panteleri, R., Sugimoto, N., Douris, V., Tirry, L., Osakabe, M., Vontas,
520 J., Van Leeuwen, T., 2017. A mutation in the PSST homologue of complex I
521 (NADH:ubiquinone oxidoreductase) from *Tetranychus urticae* is associated with resistance to
522 METI acaricides. *Insect Biochem Mol Biol* *80*, 79-90.

523

524 Betts, M.J., Russell, R.B., 2003. Amino acid properties and consequences of substitutions in:
525 Barnes, M.R., Gray, I.C. (Eds.), *Bioinformatics for Geneticists*, Wiley.

526

527 Blaazer, C.J.H., Villacis-Perez, E.A., Chafi, R., Van Leeuwen, T., Kant, M.R., Schimmel, B.C.J.,
528 2018. Why Do Herbivorous Mites Suppress Plant Defenses? *Front Plant Sci* *9*, 1057.

529
530 Bryon, A., Kurlovs, A.H., Dermauw, W., Greenhalgh, R., Riga, M., Grbić, M., Tirry, L., Osakabe,
531 M., Vontas, J., Clark, R.M., Van Leeuwen, T., 2017. Disruption of a horizontally transferred
532 phytoene desaturase abolishes carotenoid accumulation and diapause in *Tetranychus*
533 *urticae*. Proc Natl Acad Sci U S A 114, E5871-E5880.
534
535 Bryon, A., Wybouw, N., Dermauw, W., Tirry, L., Van Leeuwen, T., 2013. Genome wide gene-
536 expression analysis of facultative reproductive diapause in the two-spotted spider mite
537 *Tetranychus urticae*. BMC Genomics 14, 815.
538
539 Bui, H., Greenhalgh, R., Ruckert, A., Gill, G.S., Lee, S., Ramirez, R.A., Clark, R.M., 2018.
540 Generalist and Specialist Mite Herbivores Induce Similar Defense Responses in Maize and
541 Barley but Differ in Susceptibility to Benzoxazinoids. Front Plant Sci 9.
542
543 Chaverra-Rodriguez, D., Macias, V.M., Hughes, G.L., Pujhari, S., Suzuki, Y., Peterson, D.R.,
544 Kim, D., McKeand, S., Rasgon, J.L., 2018. Targeted delivery of CRISPR-Cas9 ribonucleoprotein
545 into arthropod ovaries for heritable germline gene editing. Nat Comm 9, 3008.
546
547 Cho, S.W., Lee, J., Carroll, D., Kim, J.-S., Lee, J., 2013. Heritable Gene Knockout in
548 *Caenorhabditis elegans* by Direct Injection of Cas9-sgRNA Ribonucleoproteins. Genetics 195,
549 1177-1180.
550
551 Concordet, J.-P., Haeussler, M., 2018. CRISPOR: intuitive guide selection for CRISPR/Cas9
552 genome editing experiments and screens. Nucleic Acids Res 46, W242-W245.
553
554 Dermauw, W., Osborne, E.J., Clark, R.M., Grbic, M., Tirry, L., Van Leeuwen, T., 2013a. A burst
555 of ABC genes in the genome of the polyphagous spider mite *Tetranychus urticae*. BMC
556 Genomics 14, 317.
557
558 Dermauw, W., Wybouw, N., Rombauts, S., Menten, B., Vontas, J., Grbic, M., Clark, R.M.,
559 Feyereisen, R., Van Leeuwen, T., 2013b. A link between host plant adaptation and pesticide
560 resistance in the polyphagous spider mite *Tetranychus urticae*. Proc Natl Acad Sci U S A 110,
561 E113-E122.
562
563 Dickinson, D.J., Goldstein, B., 2016. CRISPR-Based Methods for *Caenorhabditis elegans*
564 Genome Engineering. Genetics 202, 885-901.
565
566 Douris, V., Steinbach, D., Panteleri, R., Livadaras, I., Pickett, J.A., Van Leeuwen, T., Nauen, R.,
567 Vontas, J., 2016. Resistance mutation conserved between insects and mites unravels the
568 benzoylurea insecticide mode of action on chitin biosynthesis. Proc Natl Acad Sci U S A 113,
569 14692-14697.
570
571 Farboud, B., Severson, A.F., Meyer, B.J., 2019. Strategies for Efficient Genome Editing Using
572 CRISPR-Cas9. Genetics 211, 431-457.
573
574 Garb, J.E., Sharma, P.P., Ayoub, N.A., 2018. Recent progress and prospects for advancing
575 arachnid genomics. Curr Opin Insect Sci 25, 51-57.

576
577 Grbic, M., Van Leeuwen, T., Clark, R.M., Rombauts, S., Rouze, P., Grbic, V., Osborne, E.J.,
578 Dermauw, W., Ngoc, P.C.T., Ortego, F., Hernandez-Crespo, P., Diaz, I., Martinez, M., Navajas,
579 M., Sucena, E., Magalhaes, S., Nagy, L., Pace, R.M., Djuranovic, S., Smagghe, G., Iga, M.,
580 Christiaens, O., Veenstra, J.A., Ewer, J., Mancilla Villalobos, R., Hutter, J.L., Hudson, S.D.,
581 Velez, M., Yi, S.V., Zeng, J., Pires-daSilva, A., Roch, F., Cazaux, M., Navarro, M., Zhurov, V.,
582 Acevedo, G., Bjelica, A., Fawcett, J.A., Bonnet, E., Martens, C., Baele, G., Wissler, L., Sanchez-
583 Rodriguez, A., Tirry, L., Blais, C., Demeestere, K., Henz, S.R., Gregory, T.R., Mathieu, J.,
584 Verdon, L., Farinelli, L., Schmutz, J., Lindquist, E., Feyereisen, R., Van de Peer, Y., 2011. The
585 genome of *Tetranychus urticae* reveals herbivorous pest adaptations. *Nature* 479, 487-492.
586
587 Gui, T., Zhang, J., Song, F., Sun, Y., Xie, S., Yu, K., Xiang, J., 2016. CRISPR/Cas9-Mediated
588 Genome Editing and Mutagenesis of *EcChi4* in *Exopalaemon carinicauda*. *G3* 6, 3757-3764.
589
590 Hunter, W.B., Gonzalez, M.T., Tomich, J., 2018. BAPC-assisted CRISPR/Cas9 System: Targeted
591 Delivery into Adult Ovaries for Heritable Germline Gene Editing (Arthropoda: Hemiptera).
592 bioRxiv, 478743.
593
594 Iida, J., Desaki, Y., Hata, K., Uemura, T., Yasuno, A., Islam, M., Maffei, M.E., Ozawa, R.,
595 Nakajima, T., Galis, I., Arimura, G.-i., 2019. Tetransins: new putative spider mite elicitors of
596 host plant defense. *New Phytol* 224, 875-885.
597
598 Ismail, N.I.B., Kato, Y., Matsuura, T., Watanabe, H., 2018. Generation of white-eyed *Daphnia*
599 *magna* mutants lacking scarlet function. *PLoS One* 13, e0205609.
600
601 Jinek, M., Chylinski, K., Fonfara, I., Hauer, M., Doudna, J.A., Charpentier, E., 2012. A
602 Programmable Dual-RNA-Guided DNA Endonuclease in Adaptive Bacterial Immunity.
603 *Science* 337, 816-821.
604
605 Jonckheere, W., Dermauw, W., Zhurov, V., Wybouw, N., Van den Bulcke, J., Villarroel, C.A.,
606 Greenhalgh, R., Grbić, M., Schuurink, R.C., Tirry, L., Baggerman, G., Clark, R.M., Kant, M.R.,
607 Vanholme, B., Menschaert, G., Van Leeuwen, T., 2016. The salivary protein repertoire of the
608 polyphagous spider mite *Tetranychus urticae*: a quest for effectors. *Mol Cell Proteomics* 15,
609 3594-3613.
610
611 Khan, S.A., Reichelt, M., Heckel, D.G., 2017. Functional analysis of the ABCs of eye color in
612 *Helicoverpa armigera* with CRISPR/Cas9-induced mutations. *Sci Rep* 7, 40025.
613
614 Khila, A., Grbić, M., 2007. Gene silencing in the spider mite *Tetranychus urticae*: dsRNA and
615 siRNA parental silencing of the Distal-less gene. *Dev Genes Evol* 217, 241-251.
616
617 Korona, D., Koestler, S.A., Russell, S., 2017. Engineering the Drosophila Genome for
618 Developmental Biology. *Journal of developmental biology* 5, 16.
619
620 Kotwica-Rolinska, J., Chodakova, L., Chvalova, D., Kristofova, L., Fenclova, I., Provaznik, J.,
621 Bertolutti, M., Wu, B.C.-H., Dolezel, D., 2019. CRISPR/Cas9 Genome Editing Introduction and
622 Optimization in the Non-model Insect *Pyrrhocoris apterus*. *Front Physiol* 10.

623
624 Kurlovs, A.H., Snoeck, S., Kosterlitz, O., Van Leeuwen, T., Clark, R.M., 2019. Trait mapping in
625 diverse arthropods by bulked segregant analysis. *Curr Opin Insect Sci* 36, 57-65.
626
627 Kwon, D.H., Park, J.H., Ashok, P.A., Lee, U., Lee, S.H., 2016. Screening of target genes for
628 RNAi in *Tetranychus urticae* and RNAi toxicity enhancement by chimeric genes. *Pestic*
629 *Biochem Physiol* 130, 1-7.
630
631 Macias, V.M., McKeand, S., Chaverra-Rodriguez, D., Hughes, G.L., Fazekas, A., Pujhari, S.,
632 Jasinskiene, N., James, A.A., Rasgon, J.L., 2019. Cas9-mediated gene-editing in the malaria
633 mosquito *Anopheles stephensi* by ReMOT Control. bioRxiv, 775312.
634
635 Maoka, T., 2019. Carotenoids as natural functional pigments. *Journal of Natural Medicines*.
636
637 Martel, C., Zhurov, V., Navarro, M., Martinez, M., Cazaux, M., Auger, P., Migeon, A.,
638 Santamaria, M.E., Wybouw, N., Diaz, I., 2015. Tomato Whole Genome Transcriptional
639 Response to *Tetranychus urticae* Identifies Divergence of Spider Mite-Induced Responses
640 Between Tomato and Arabidopsis. *Mol Plant Microbe Interact* 28, 343-361.
641
642 Martin, A., Serano, J.M., Jarvis, E., Bruce, H.S., Wang, J., Ray, S., Barker, C.A., O'Connell, L.C.,
643 Patel, N.H., 2016. CRISPR/Cas9 mutagenesis reveals versatile roles of Hox genes in
644 crustacean limb specification and evolution. *Curr Biol* 26, 14-26.
645
646 Mota-Sanchez, R.M., Wise, J.C., 2019. Arthropod Pesticide Resistance Database (APRD).
647 Available at: <https://www.pesticideresistance.org/>.
648
649 Muller, H.J., 1932. Further studies on the nature and causes of gene mutations. *Proceedings*
650 *of the Sixth International Congress of Genetics, Ithaca, New York.* 1, 213-255.
651
652 Nakanishi, T., Kato, Y., Matsuura, T., Watanabe, H., 2014. CRISPR/Cas-Mediated Targeted
653 Mutagenesis in *Daphnia magna*. *PLoS One* 9, e98363.
654
655 Navajas, M., Lagnel, J., Gutierrez, J., Boursot, P., 1998. Species-wide homogeneity of nuclear
656 ribosomal ITS2 sequences in the spider mite *Tetranychus urticae* contrasts with extensive
657 mitochondrial COI polymorphism. *Heredity* 80, 742-752.
658
659 Prado-Cabrero, A., Schaub, P., Díaz-Sánchez, V., Estrada, A.F., Al-Babili, S., Avalos, J., 2009.
660 Deviation of the neurosporaxanthin pathway towards β -carotene biosynthesis in *Fusarium*
661 *fujikuroi* by a point mutation in the phytoene desaturase gene. *The FEBS Journal* 276, 4582-
662 4597.
663
664 Presnail, J.K., Hoy, M.A., 1992. Stable genetic transformation of a beneficial arthropod,
665 *Metaseiulus occidentalis* (Acari: Phytoseiidae), by a microinjection technique. *Proc Natl Acad*
666 *Sci U S A* 89, 7732-7736.
667
668 Reardon, S., 2019. CRISPR gene-editing creates wave of exotic model organisms. *Nature* 568,
669 441-442

670
671 Riga, M., Bajda, S., Themistokleous, C., Papadaki, S., Palzewicz, M., Dermauw, W., Vontas, J.,
672 Leeuwen, T.V., 2017. The relative contribution of target-site mutations in complex acaricide
673 resistant phenotypes as assessed by marker assisted backcrossing in *Tetranychus urticae*. *Sci*
674 *Rep* 7, 9202.
675
676 Rozen, S., Skaletsky, H.J., 2000. Primer3 on the WWW for general users and for biologist
677 programmers, in: Krawetz, S., Misener, S. (Eds.), *Bioinformatics Methods and Protocols:*
678 *Methods in Molecular Biology*. Humana Press, Totowa, New Jersey, USA, pp. 365-386.
679
680 Rungger, D., Muster, L., Georgiev, O., Rungger-Brändle, E., 2017. Oocyte shuttle, a
681 recombinant protein transporting donor DNA into the *Xenopus* oocyte *in situ*.
682 *Biology Open* 6, 290-295.
683
684 Rusk, N., 2019. Spotlight on Cas12. *Nat Meth* 16, 215-215.
685
686 Santamaría, M.E., Hernández-Crespo, P., Ortego, F., Grbic, V., Grbic, M., Diaz, I., Martinez,
687 M., 2012. Cysteine peptidases and their inhibitors in *Tetranychus urticae*: a comparative
688 genomic approach. *BMC Genomics* 13, 307.
689
690 Santamaría, M.E., Martínez, M., Arnaiz, A., Rioja, C., Burow, M., Grbic, V., Díaz, I., 2019. An
691 Arabidopsis TIR-Lectin Two-Domain Protein Confers Defense Properties against *Tetranychus*
692 *urticae*. *Plant Physiol* 179, 1298-1314.
693
694 Sanz, C., Alvarez, M.I., Orejas, M., Velayos, A., Eslava, A.P., Benito, E.P., 2002. Interallelic
695 complementation provides genetic evidence for the multimeric organization of the
696 *Phycomyces blakesleeanus* phytoene dehydrogenase. *Eur J Biochem* 269, 902-908.
697
698 Schlachter, C.R., Daneshian, L., Amaya, J., Klapper, V., Wybouw, N., Borowski, T., Van
699 Leeuwen, T., Grbic, V., Grbic, M., Makris, T.M., Chruszcz, M., 2019. Structural and functional
700 characterization of an intradiol ring-cleavage dioxygenase from the polyphagous spider mite
701 herbivore *Tetranychus urticae* Koch. *Insect Biochem Mol Biol* 107,
702 doi:10.1016/j.ibmb.2018.1012.1001.
703
704 Scott, J.G., Michel, K., Bartholomay, L.C., Siegfried, B.D., Hunter, W.B., Smagghe, G., Zhu,
705 K.Y., Douglas, A.E., 2013. Towards the elements of successful insect RNAi. *J Insect Physiol* 59,
706 1212-1221.
707
708 Scott, M.J., Gould, F., Lorenzen, M., Grubbs, N., Edwards, O., O'Brochta, D., 2018.
709 Agricultural production: assessment of the potential use of Cas9-mediated gene drive
710 systems for agricultural pest control. *Journal of Responsible Innovation* 5, S98-S120.
711
712 Sharma, A., 2017. Development of CRISPR-Cas9 gene drive system for deer tick, *Ixodes*
713 *scapularis*, IGTRCN Peer-to-Peer Training Fellowship Report. Available at:
714 http://igtrcn.org/wp-content/uploads/2018/01/Sharma_IGTRCN_report_val.docx, University
715 of Maryland, MD, USA.
716

- 717 Snoeck, S., Wybouw, N., Van Leeuwen, T., Dermauw, W., 2018. Transcriptomic Plasticity in
718 the Arthropod Generalist *Tetranychus urticae* Upon Long-Term Acclimation to Different Host
719 Plants. *G3* 8, 3865-3879.
- 720
- 721 Sun, D., Guo, Z., Liu, Y., Zhang, Y., 2017. Progress and prospects of CRISPR/Cas systems in
722 insects and other arthropods. *Front Physiol* 8, 608.
- 723
- 724 Suzuki, T., Nunes, M.A., España, M.U., Namin, H.H., Jin, P., Bensoussan, N., Zhurov, V.,
725 Rahman, T., De Clercq, R., Hilson, P., Grbic, V., Grbic, M., 2017. RNAi-based reverse genetics
726 in the chelicerate model *Tetranychus urticae*: A comparative analysis of five methods for
727 gene silencing. *PLoS One* 12, e0180654.
- 728
- 729 Van Leeuwen, T., Demaeght, P., Osborne, E.J., Dermauw, W., Gohlke, S., Nauen, R., Grbic,
730 M., Tirry, L., Merzendorfer, H., Clark, R.M., 2012. Population bulk segregant mapping
731 uncovers resistance mutations and the mode of action of a chitin synthesis inhibitor in
732 arthropods. *Proc Natl Acad Sci U S A* 109, 4407-4412.
- 733
- 734 Van Leeuwen, T., Dermauw, W., 2016. The molecular evolution of xenobiotic metabolism
735 and resistance in Chelicerate mites. *Annu Rev Entomol* 61, 475-498.
- 736
- 737 Van Leeuwen, T., Tirry, L., Yamamoto, A., Nauen, R., Dermauw, W., 2015. The economic
738 importance of acaricides in the control of phytophagous mites and an update on recent
739 acaricide mode of action research. *Pestic Biochem Physiol* 121, 12-21.
- 740
- 741 Villarroel, C.A., Jonckheere, W., Alba, J.M., Glas, J.J., Dermauw, W., Haring, M.A., Van
742 Leeuwen, T., Schuurink, R.C., Kant, M.R., 2016. Salivary proteins of spider mites suppress
743 defenses in *Nicotiana benthamiana* and promote mite reproduction. *Plant J* 86, 119-131.
- 744
- 745 Witte, H., Moreno, E., Rödelsperger, C., Kim, J., Kim, J.-S., Streit, A., Sommer, R.J., 2015.
746 Gene inactivation using the CRISPR/Cas9 system in the nematode *Pristionchus pacificus*. *Dev*
747 *Genes Evol* 225, 55-62.
- 748
- 749 Wybouw, N., Balabanidou, V., Ballhorn, D.J., Dermauw, W., Grbić, M., Vontas, J., Van
750 Leeuwen, T., 2012. A horizontally transferred cyanase gene in the spider mite *Tetranychus*
751 *urticae* is involved in cyanate metabolism and is differentially expressed upon host plant
752 change. *Insect Biochem Mol Biol* 42, 881-889.
- 753
- 754 Wybouw, N., Dermauw, W., Tirry, L., Stevens, C., Grbic, M., Feyereisen, R., Van Leeuwen, T.,
755 2014. A gene horizontally transferred from bacteria protects arthropods from host plant
756 cyanide poisoning. *Elife* 3, e02365.
- 757
- 758 Wybouw, N., Kosterlitz, O., Kurlovs, A.H., Bajda, S., Greenhalgh, R., Snoeck, S., Bui, H., Bryon,
759 A., Dermauw, W., Van Leeuwen, T., Clark, R.M., 2019a. Long-Term Population Studies
760 Uncover the Genome Structure and Genetic Basis of Xenobiotic and Host Plant Adaptation in
761 the Herbivore *Tetranychus urticae*. *Genetics*, doi: 10.1534/genetics.1118.301803
- 762

763 Wybouw, N., Kurlovs, A.H., Greenhalgh, R., Bryon, A., Kosterlitz, O., Manabe, Y., Osakabe,
764 M., Vontas, J., Clark, R.M., Leeuwen, T.V., 2019b. Convergent evolution of cytochrome P450s
765 underlies independent origins of keto-carotenoid pigmentation in animals. Proceedings of
766 the Royal Society B: Biological Sciences 286, 20191039.

767

768 Wybouw, N., Van Leeuwen, T., Dermauw, W., 2018. A massive incorporation of microbial
769 genes into the genome of *Tetranychus urticae*, a polyphagous arthropod herbivore. Insect
770 Mol Biol 27, 333-351.

771

772 Wybouw, N., Zhurov, V., Martel, C., Bruinsma, K.A., Hendrickx, F., Grbić, V., Van Leeuwen, T.,
773 2015. Adaptation of a polyphagous herbivore to a novel host plant extensively shapes the
774 transcriptome of herbivore and host. Mol Ecol 24, 4647-4663.

775

776 Xue, W.-H., Xu, N., Yuan, X.-B., Chen, H.-H., Zhang, J.-L., Fu, S.-J., Zhang, C.-X., Xu, H.-J., 2018.
777 CRISPR/Cas9-mediated knockout of two eye pigmentation genes in the brown planthopper,
778 *Nilaparvata lugens* (Hemiptera: Delphacidae). Insect Biochem Mol Biol 93, 19-26.

779

780 Zhang, L., Reed, R.D., 2017. A Practical Guide to CRISPR/Cas9 Genome Editing in Lepidoptera,
781 in: Sekimura, T., Nijhout, H.F. (Eds.), Diversity and Evolution of Butterfly Wing Patterns: An
782 Integrative Approach. Springer Singapore, Singapore, pp. 155-172.

783

784 Zhao, C., Nability, P.D., 2017. Phylloxerids share ancestral carotenoid biosynthesis genes of
785 fungal origin with aphids and adelgids. PLoS One 12, e0185484.

786

787 Zhurov, V., Navarro, M., Bruinsma, K.A., Arbona, V., Estrella Santamaria, M., Cazaux, M.,
788 Wybouw, N., Osborne, E.J., Ens, C., Rioja, C., Vermeirssen, V., Rubio-Somoza, I., Krishna, P.,
789 Diaz, I., Schmid, M., Gomez-Cadenas, A., Van de Peer, Y., Grbic, M., Clark, R.M., Van
790 Leeuwen, T., Grbic, V., 2014. Reciprocal responses in the interaction between *Arabidopsis*
791 and the cell-content-feeding chelicerate herbivore spider mite. Plant Physiol 164, 384-399.

792

793

794

795

796

797

798

799

800

801

802

803

804

805

806

807

808 **Tables**

809

Table 1 - CRISPR-Cas9 efficiency

	injection batch	
	A	B
number of injected virgin females	245	177
number of injected virgin females alive after 24h	192	127
number of CRISPRed albino male offspring alive*	1	1
number of CRISPRed albino male offspring not alive**	13	0
% CRISPR-Cas9 success	5.71	0.56

*all alive offspring were found in the first 24h after injection

**assuming albino phenotype is caused by a CRISPR-Cas9 event; all collected dead offspring were either in the protonymph or protochrysalis stage

810

811

812

813

814

815

816

817

818

819

820

821

822

823

824

825

826

827

828

829

830

831

832

833

834

835

Table 2 - Inheritance and complementation tests

Crosses	F ₁ ♂, % albino?	F ₂ haploid males		χ^2	P value
		ALB	WT		
<i>Inheritance tests (female x male)*</i>					
WT x CRISPR A (rep1)	0	15	20	0.714	0.39802
WT x CRISPR A (rep2)	0	30	21	1.588	0.20758
WT x CRISPR A (rep3)	0	17	20	0.243	0.62187
WT x CRISPR B (rep1)	0	25	20	0.556	0.45606
WT x CRISPR B (rep2)	0	12	14	0.154	0.69489
WT x CRISPR B (rep3)	0	28	27	0.018	0.89274
<i>Complementation tests (female x male)**</i>					
CRISPR A x Alb-NL***	100				
CRISPR B x Alb-NL	100				
CRISPR A x CRISPR B	100				

*an alive albino male - CRISPR A or CRISPR B - that was detected in the progeny of Cas9-sgRNA injected females of either batch A or B, respectively, was crossed with three to five females of the WT strain (1 male x 3-5 females) in 3 replicates

** 15 females crossed with 30 males; 100 F₁ females were screened for wildtype or albino phenotype

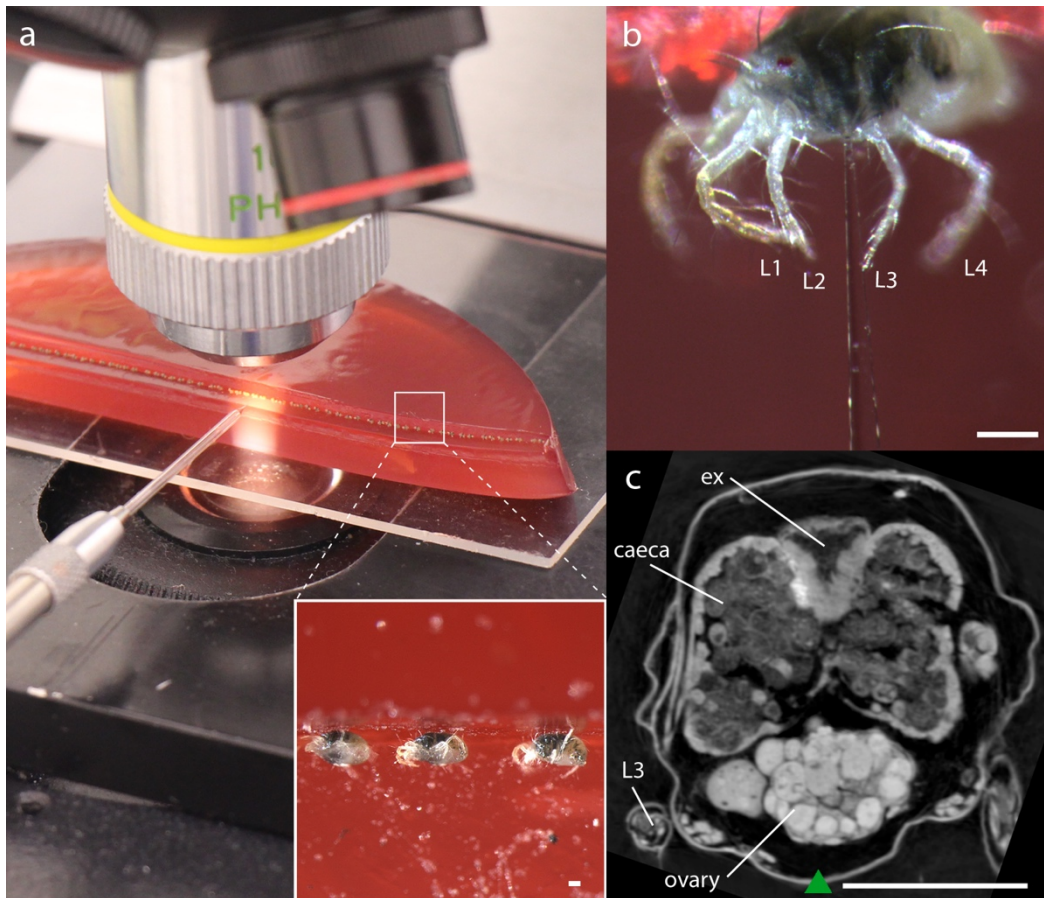
*** the Alb-NL strain is an albino *T. urticae* strain known to have an inactivating mutation in its carotenoid desaturase gene (*tetur01g11270*) (Bryon et al. 2017)

836
837
838
839
840
841
842
843
844
845
846
847
848
849
850
851
852
853
854
855
856
857
858
859

860 **Figures**

861

862



863

864

865 **Figure 1 - Cas9-sgRNA micro-injection setup for *T. urticae***

866 (a) setup for injection of *T. urticae* females: virgin females were aligned on an “agar platform”
867 and injected under a microscope; insert: mites aligned on the agar platform, (b) females
868 approximately injected at the third pair of legs: L1, L2, L3 and L4 refer to the 1st, 2nd, 3rd and
869 4th pair of legs, respectively (c) virtual cross-section at the third pair of legs; this section was
870 obtained from a previously performed submicron CT scan of a *T. urticae* adult female
871 (Jonckheere et al., 2016); a green triangle points towards Cas9-sgRNA injection location; L3:
872 third pair of legs, ex= excretory organ. Scale bar in each panel represents 0.1 mm.

873

874

875

876

877

878

879

880

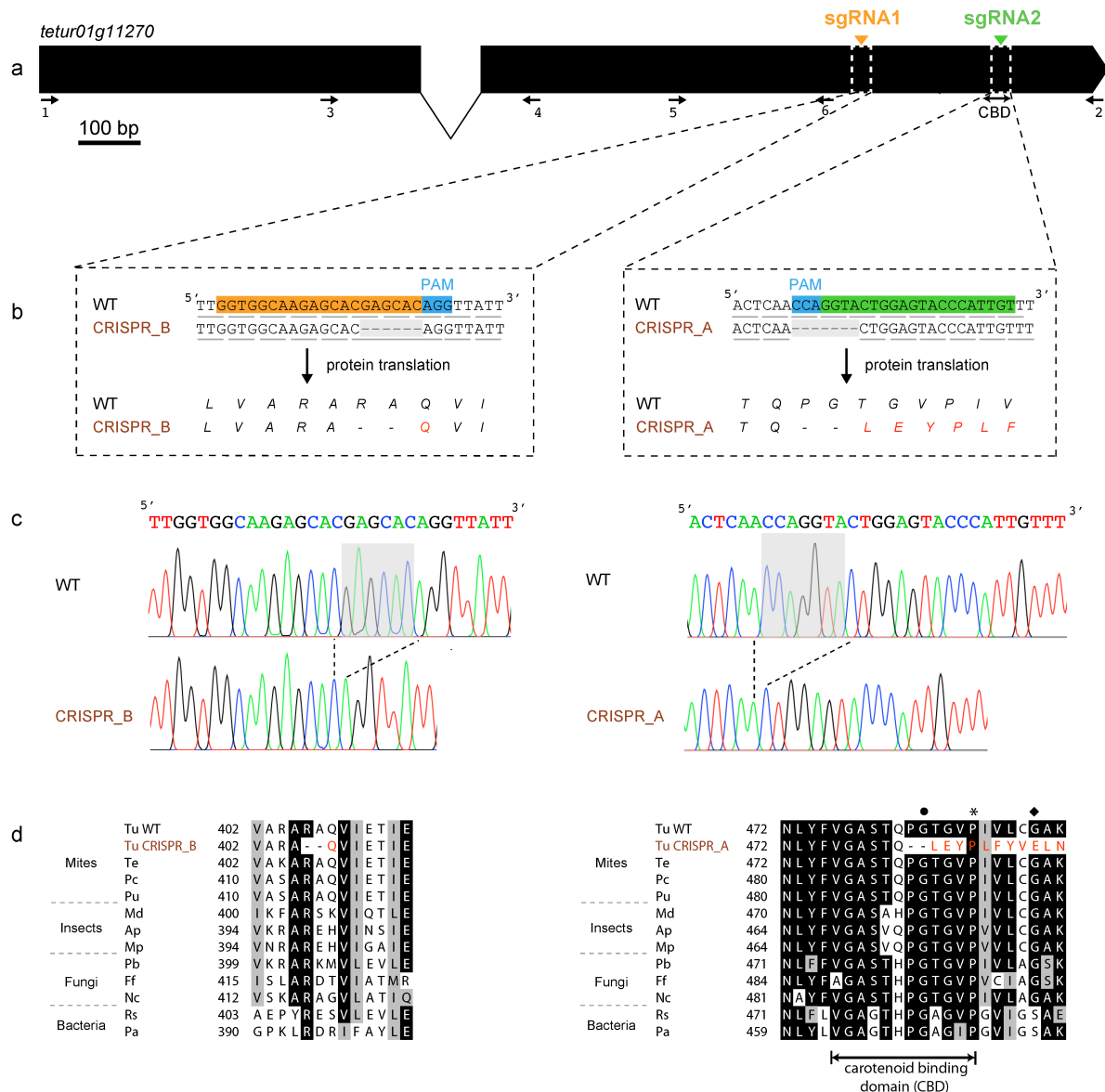
881



882
883

884 **Figure 2 - Phenotypes of adult *T. urticae* females of the WT strain, CRISPR line A and B**
885 Shown are (a) *T. urticae* pigmentation of the WT strain, (b) albino phenotype of CRISPR line A
886 and (c) albino phenotype of CRISPR line B. In all cases, adult females are shown. Arrows
887 indicate red eye spots or distal red-orange pigmentation in the forelegs of WT mites, which
888 are absent in albino females of line A, while females of line B have no red pigmentation in the
889 forelegs but slight traces of red pigmentation (here barely visible) are present in the eyes. Left:
890 lateral view; Right: dorsal view. Scale bar represents 0.1 mm.

891
892
893
894
895
896
897



898

899 **Figure 3 - Small indels detected in the phytoene desaturase gene (*tetur01g11270*) of *T.***
 900 ***urticae* females of CRISPR line A and B**

901 (a) gene structure of *tetur01g11270*; the position of sgRNA1 and sgRNA2 cutting sites are
 902 indicated with an orange and green triangle, respectively; the position of the primers (1-6)
 903 used for PCR and sequencing of *tetur01g11270* cDNA is indicated with arrows (Table S2); (b)
 904 indels found adjacent to the sgRNA cutting sites in *tetur01g11270* of females of CRISPR line A
 905 or B; the guide sequence of sgRNA1 and the reverse complement of the sgRNA2 guide
 906 sequence are highlighted in orange and green, respectively, while the protospacer adjacent
 907 motif (PAM) is highlighted in blue; codons are underlined; (b-left) a 6 bp deletion (shaded gray)
 908 was found in *tetur01g11270* of females of CRISPR line B, resulting in the deletion of two
 909 amino acids; (b-right) a 7 bp deletion (shaded gray) was found in females from CRISPR line A,
 910 causing a deletion of two amino acids in the carotenoid binding domain and a frame shift
 911 changing translation; (c) chromatogram of the sequences displayed in (b), with the deletions
 912 present in the CRISPR lines shaded gray; (d) alignment of *tetur01g11270* of CRISPR line B (d-

913 left) and CRISPR line A (d-right) with those of other tetranychid mites (*Te*, *Tetranychus evansi*,
914 *Pu*, *Panonychus citri*, *Pc*, *Panonychus ulmi*), insects (*Md*, *Mayetiola destructor*, *Ap*,
915 *Acyrtosiphon pisum*, *Mp*, *Myzus persicae*), Fungi (*Pb*, *Phycomyces blakesleeanus*, *Ff*, *Fusarium*
916 *fujikuroi* and *Nc*, *Neurospora crassa*) and Bacteria (*Rs*, *Rhodobacter sphaeroides* and *Pa*,
917 *Pantoea ananatis*). Accession numbers of all sequences can be found in Bryon et al. (2017)
918 and in Supplementary Figure S6. (d-right) Mutations in *P. blakesleeanus* and *F. fujikuroi* that
919 result in lowered phytoene desaturase activities are indicated with a black dot and rhombus,
920 respectively (Prado-Cabrero et al., 2009; Sanz et al., 2002), while a Pro487Leu mutation that
921 was identified in *tetur01g11270* of *T. urticae* lines W-Alb-1/W-Alb-2, with young stages lacking
922 pigment but red color being apparent in adults (Bryon et al., 2017), is indicated with an
923 asterisk.

924

925 **Supplementary Figure Legends**

926

927 **Figure S1 - Agar platforms used for injection of *T. urticae* females**

928 (a) two microscopic slides attached to each other; (b) cherry/agar plate containing the two
929 microscope slides; after solidification of agar, slides were removed from the agar and the agar
930 plate was cut in two along the length of the slide indentation.

931

932 **Figure S2 - Injection needle used for injections of *T. urticae* females.** (a) injection needle
933 pulled from Clark capillary glass; scale bar represents 0.1 mm (b) close-up of the tip of the
934 pulled needle.

935

936 **Figure S3 - *In vitro* digestion with Cas9/sgRNAs of two PCR amplicons of *tetur01g11270* of**
937 **adult females of the *T. urticae* WT strain.** lane 1: Cas9 with PCR amplicon 1 (895 bp); lane 2:
938 Cas9 with PCR amplicon 1 and sgRNA1, resulting in a 537 bp and 398 bp fragment (black
939 arrows); lane 3: Cas9 with PCR amplicon 2 (699 bp); lane 4: Cas9 with PCR amplicon 2 and
940 sgRNA2 resulting in a 502 bp and 197 bp fragment (white arrows); M: BenchTop 100 bp DNA
941 ladder (Promega, catalog# G8291).

942

943 **Figure S4 - Phenotype of immature stages of the *T. urticae* WT strain and CRISPR lines A and**
944 **B.** Shown are (a) *T. urticae* pigmentation of the WT strain, (b) albino phenotype of CRISPR line
945 A and (c) albino phenotype of CRISPR line B. In (a) and (c) larval stages are shown while in (b)
946 a protonymphal stage is shown. Arrows indicate red eye spots of WT mites that are absent in
947 immature stages of line A and B. Scale bar represents 0.1 mm.

948

949 **Figure S5 - Phenotype of adult males of the *T. urticae* WT strain and CRISPR lines A and B.**
950 Shown are (a) *T. urticae* pigmentation of the WT strain, (b) albino phenotype of CRISPR line A
951 and (c) albino phenotype of CRISPR line B. Arrows indicate red eye spots of WT mites that are
952 absent in males of line A, while traces of red pigment can be seen in the eyes of males of line
953 B. Scale bar represents 0.1 mm.

954

955 **Figure S6 - Nucleotide alignment of cDNA of *tetur01g11270* of the *T. urticae* WT strain and**
956 **CRISPR line A and B.** Nucleotides with 100% identity are shaded black; *tetur01g11270* of
957 CRISPR B line was completely identical to *tetur01g11270* of the WT strain while three non-
958 synonymous SNPs (indicated in blue font) were found in *tetur01g11270* cDNA of the A strain.

959

960 **Figure S7 - Alignment of *tetur01g11270*, *tetur11g04810* and *tetur11g04820* of the London**
961 **strain (Grbic et al. 2011) with guide sequences of sgRNA1 and sgRNA2.** Guide sequences of
962 sgRNA1 and sgRNA2 are shaded orange and green respectively.

963

964 **Supplementary Tables**

965

966 **Table S1 - Composition of CRISPR-Cas9 injection mix**

967

968 **Table S2 - Primers used in this study**

969